

An Object Tracking Algorithm For Echocardiogram Images

B. Acharya Jayanta Mukherjee A. K. Majumdar
Department of Computer Science and Engineering
Indian Institute of Technology, Kharagpur, INDIA

Abstract

In this work we present a technique for tracking contours from echocardiogram video. Our aim is to calculate area of a heart chamber, say, left ventricle(LV), over time from the video. To do so, we have tried to estimate LV boundary by an ellipse for each frame. The system requires a user drawn ellipse describing the LV in the first frame. For the next frames, this ellipse is adjusted according to the movement of the LV. Tracking of this movement is done using edge information of LV. Finally, in all frames, the elliptic contour is allowed to converge to the desired boundary using active contouring principle.

1 Introduction

In last few decades, medical imaging techniques have seen rapid progress. However, automated analysis and interpretation of these images are far away from the expectation. One of the major problems in medical image analysis is delineation of objects, like cells, organs, boundaries of different cavities. In particular, for ischemic heart diseases, echocardiography is useful in diagnosis of myocardial infarction and transient ischemic episodes. The analysis of echocardiographic image sequences is usually performed by visual inspection. However, some systems are able to delineate heart cavities and to estimate some useful parameters [1] [2]. A survey of related work is also available in [3]. In this work, we have proposed a method to track the deformation of left ventricle (LV) wall motion with an objective to predict the area changes of LV. The major approaches in this direction use interpolation of edge pixels [4], snakes [5], segmentation based on Markov Random Fields [6] and Optical Flow [7]. Nevertheless, these techniques in echocardiogram images suffer mainly from usual poor quality of images. Also, they are computationally intensive [2]. In [2], a technique using constrained tracking has been proposed. The major drawback of this method is that the set of parameters used are to be tuned by cardiologist.

In our approach, we have tried to achieve two goals:

to provide an area-plot of cardiac cavities over the time, and to minimise user interaction to use the system, so that the system can be used as an assisting tool for diagnosis. To start with, we have adopted a simple heuristic to obtain a good initial estimate of the boundary. Then, this contour is refined using active contouring [8] based relaxation technique for extraction of cavity boundary from an echocardiogram image. Finally, to track the movement over time of this cavity, we are using the information of cavity boundary of one of the previous frames. A plot of the change in area of the cavity is generated to extract information about expansion - contraction pattern of left ventricle. In the present work, we have considered the extraction of the closed contours only.

The rest of the paper is organised in the following manner. In section 2, we have given brief description of the algorithm used to extract contours of cavities from echocardiogram images. In section 3, a refinement of the method has been discussed. In section 4, we have shown some experimental results.

2 Contour Estimation

Echocardiogram images are used by cardiologists to analyse physiological and functional behaviour of cardiovascular components, e.g. heart chambers, valves, arteries etc. In that process, heart chamber can be viewed through different angles by changing the transducer position. Accordingly, same chamber can be seen in different perspectives, known as *views*. For analysis of LV, one such important *view* is short-axis view, as shown in Fig. 1. In this work, LV areas are computed from echocardiogram images of short-axis view. In our earlier work [9], we ensured the inner area of the cavity using a two-phase relaxation method based on active contouring. Similar approach, to extract boundary of objects was also reported in [10]. However, the method failed to extract the true boundary due to the presence of papillary muscles and valves. This can be seen in Fig. 1(b). To deal with this problem, we observed that, in short-axis view LV appears in elliptical shape. This observation

has motivated us to model LV as an ellipse. Thus, an ellipse is drawn by the user close to the LV boundary in an echocardiogram frame. This ellipse is then allowed to converge locally to the actual contour using relaxation as described in [9].

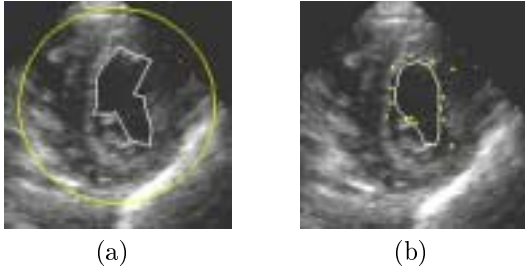


Figure 1: (a) initial contour (b) final contour

However, to find area of the cavity, over time, it is not possible to use the same ellipse (user input). The reason behind this is the fact that, heart chambers undergo rigid and non-rigid motion throughout a cardiac cycle. Also, during the process of capturing echocardiogram video, the transducer, held by the operator, moves relative to the patient's body. These factors cause an unpredictable motion of heart chambers and can be observed clearly from an echocardiogram video sequence. To deal with this problem, the user given ellipse is adjusted in each of the succeeding frames and is then allowed to converge to final contour.

2.1 Contour Initialisation

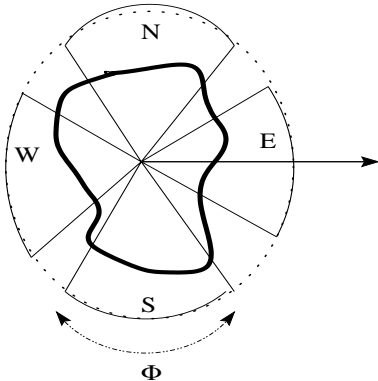


Figure 2: Angular division of control points

In a cardiac motion, LV goes through a periodic change in shape and size. The phase when LV is fully expanded is called *end diastole* (ED) and the phase

when it is fully contracted, is called *end systole* (ES). Thus, LV starts contracting from ED till it reaches ES, and from ES it starts expanding to reach finally to ED. The time span between one ED and next ED or between one ES and next ES is termed as a *cardiac cycle*. In our technique, we assume that user provides an ellipse in one of the ED frames of the video. This requirement is not a major restriction of our method, but is imposed to estimate the maximum possible size of LV in an echocardiogram video. Thus, in our implementation, user draws two lines on the object of interest, one in vertical direction and one in horizontal direction, representing the major axis and minor axis of the initial ellipse respectively. Let $v_s(x_1, y_1)$ and $v_e(x_2, y_2)$ be the starting point and ending point of the vertical line respectively. Similarly, let $h_s(x_3, y_3)$ and $h_e(x_4, y_4)$ be the starting point and ending point of horizontal line respectively. In general, $x_1 \neq x_2$ and $y_3 \neq y_4$, as the lines are manually drawn by dragging a mouse. In Cartesian coordinate system, $y_1 > y_2$ and $x_3 < x_4$. Then, the centre of the ellipse $C(x_c, y_c)$ is defined as,

$$(x_c, y_c) = \left(\frac{x_3 + x_4}{2}, \frac{y_1 + y_2}{2} \right) \quad (1)$$

The semi-major axis a and the semi-minor axis b are calculated as,

$$a = (y_1 - y_2)/2, \quad b = (x_4 - x_3)/2 \quad (2)$$

Finally, a set of points (ex_k, ey_k) is generated by the formula,

$$(ex_k, ey_k) = (x_c + a \cos(k\theta), y_c + b \sin(k\theta)) \quad (3)$$

where, $1 \leq k \leq n$, n is the number of control points to be used for the ellipse and is given as input, and $\theta = \frac{2\pi}{n}$ in radian. $\theta = 0$ direction is shown by the horizontal arrow in Fig. 2. Ellipse, thus obtained for the first frame, and the points of that ellipse, will be denoted by \mathcal{E} and $\mathcal{E}(i)$, $1 \leq i \leq n$, respectively in rest of the paper. For any other frame, \mathcal{E}_j represents the ellipse of the j th frame. This initial estimate \mathcal{E} of the contour is then locally converged, in a number of steps, to the desired solution by minimising an energy function as described in [9]. The area of the final contour is calculated in number of pixels forming the interior.

2.2 Contour Adjustment

In this section, we discuss the scheme for adjustment of ellipse \mathcal{E} for rest of the frames. At first, we scan the edge space of the first frame radially from the centre C of ellipse \mathcal{E} to its boundary. The method

was adopted from [9]. This generates a sequence of n points maintaining the order same as that of points $\mathcal{E}(i)$. We call these points as $\hat{\mathcal{E}}(i)$, $1 \leq i \leq n$. We take the horizontal line marked with arrow in Fig. 2 as *reference line*. Let ϕ be a given angle, say $\frac{\Pi}{4}$. Let us consider the points of $\hat{\mathcal{E}}(i)$ that lie within an angular section $\frac{\phi}{2}$ on both sides of the *reference line*. We call these points as $\hat{\mathcal{E}}^E(i)$. The superscript E is used to describe the East direction (see Fig. 2). Now, we move the *reference line* by angles $\frac{\Pi}{2}, \Pi$ and $\frac{3\Pi}{2}$ and consider points of $\hat{\mathcal{E}}(i)$, in each position, symmetrically lying within angular section ϕ about the *reference line*. We denote these sets of points by $\hat{\mathcal{E}}^N(i)$, $\hat{\mathcal{E}}^W(i)$, $\hat{\mathcal{E}}^S(i)$ for North, West and South directions respectively.

In a similar manner, we find the points $\hat{\mathcal{E}}_2^E(i)$, $\hat{\mathcal{E}}_2^N(i)$, $\hat{\mathcal{E}}_2^W(i)$, $\hat{\mathcal{E}}_2^S(i)$, for the 2nd frame keeping the centre as (x_c, y_c) . Here, we assume that the cavity boundary does not move much compared to its position in the previous frame. In the following, we use the superscript d to represent the direction E, N, W, S . Next, we calculate Euclidian distance of all the points of each of the sets $\hat{\mathcal{E}}^d(i)$ from the centre C . Let us denote the medians of these distances by $\mathcal{D}^E, \mathcal{D}^N, \mathcal{D}^W, \mathcal{D}^S$ for each direction stated above. Similarly, we calculate the median distances \mathcal{D}_2^d for the points $\hat{\mathcal{E}}_2^d(i)$, from its centre. Intuitively, the differences between the median distances of successive frames are the measures of average shifts of the points of \mathcal{E} , on its axes, in the respective directions. Thus, these are used to measure the motion of the heart cavity between two successive frames. Hence, we define the general term $\Delta_{j,j+1}^d$ to represent the difference between \mathcal{D}_{j+1}^d and \mathcal{D}_j^d . However, due to the absence of an edge of the cavity or in the presence of a *weak edge*(see [9]), the quantity Δ may be large in some cases and hence, may lead to an erroneous estimation of cavity motion. To restrict that, we introduced a parameter λ and define $\Delta_{j,j+1}^d$ as below,

$$\Delta_{j,j+1}^d = \begin{cases} \lambda \mathcal{D}_j^d & \text{if } \mathcal{D}_{j+1}^d > \lambda \mathcal{D}_j^d \\ \mathcal{D}_{j+1}^d - \mathcal{D}_j^d & \text{otherwise} \end{cases} \quad (4)$$

In the context of our discussion made above, we calculate $\Delta_{1,2}^d$ and we have kept λ as 1.5. Accordingly, the points v_s, v_e, h_s, h_e are re-defined as,

$$v_s \equiv (x_c, y_c + \Delta_{1,2}^N), v_e \equiv (x_c, y_c - \Delta_{1,2}^S) \quad (5)$$

$$h_s \equiv (x_c - \Delta_{1,2}^W, y_c), h_e \equiv (x_c + \Delta_{1,2}^E, y_c) \quad (6)$$

The new centre is then calculated by Equation(1), new semi-major and semi-minor axes are found by Equation(2) and finally, the ellipse for the second

frame, \mathcal{E}_2 , is formed by Equation(3). Finally, the points $\mathcal{E}_2(i)$ are converged to the final boundary of the second frame.

Likewise, we estimate the LV area for all the frames of an echocardiogram sequence and generate an area-plot. The above method of adjusting initial ellipse is described in the following steps.

Algorithm *Init_Contour_Adjust*

Input: Echocardiogram frames f_j , $j = 1 \dots p$, number of points on ellipse(n), ϕ , λ , v_s, v_e, h_s, h_e
Output: Initial contour points $\mathcal{E}_j(i)$, $\forall j \in \{2, \dots, p\}$ and $i = 1, 2, \dots, n$

Begin

1. Calculate $C(x_c, y_c)$, a , b for the first frame by eqns.(1),(2).
2. Generate points $\mathcal{E}_1(i)$ by eqn.(2).
3. $\forall j \in \{1, \dots, p-1\}$, carry out the following steps from 4 to 7.
4. Generate points $\hat{\mathcal{E}}_j(i)$
5. $\forall d \in \{E, N, W, S\}$,
 - (a) Determine points $\hat{\mathcal{E}}_j^d(i)$.
 - (b) Generate points $\hat{\mathcal{E}}_{j+1}^d(i)$ and $\hat{\mathcal{E}}_{j+1}^d(i)$.
 - (c) Compute $\Delta_{j,j+1}^d$ by eqn.(4).
6. Adjust $C_{j+1}, a_{j+1}, b_{j+1}$ by eqns (1),(2),(5),(6).
7. Generate points $\mathcal{E}_{j+1}(i)$.

End *Init_Contour_Adjust*

3 Correlation Based Synchronisation of User's Input

It has been observed that, due to the presence of pappillary muscles, other artifacts and speckled noise within the cavity, determination of $\hat{\mathcal{E}}(i)$ becomes inaccurate in some frames. This error component, in turn, gets propagated in the subsequent computation stages leading to erroneous results in a few cases. To address this problem, we employed a method of initialising the user given ellipse input in every end diastole(ED) frame. The automatic determination of ED frames of an echocardiogram image sequence is done by using the correlation coefficient of two frames. The technique is described in the following subsections.

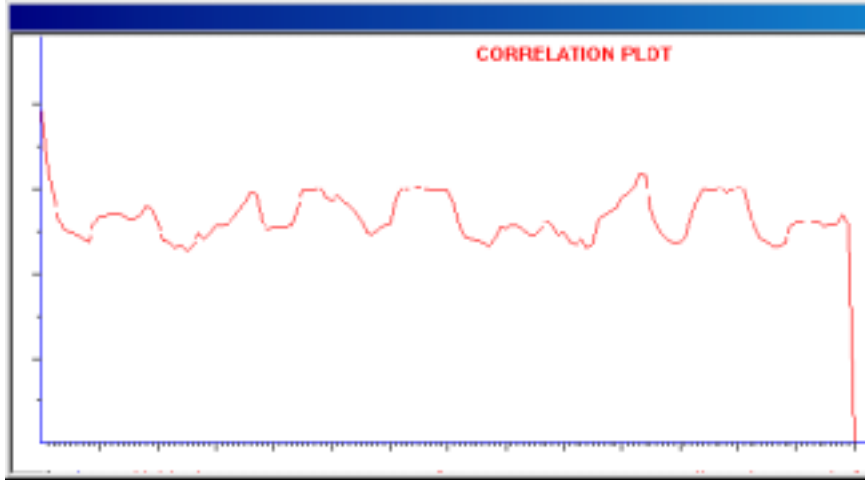


Figure 3: Correlation plot of 140 frames

3.1 Correlation Map of Image Sequences

Let us consider two static frames f_1^{ED} and f_2^{ED} of an echo sequence, describing the ED phases of two different cardiac cycles. Hence, it is expected that these two static frames will bear some amount of statistical correlation with respect to the image properties. To describe this behaviour, we define the *correlation coefficient* ρ as,

$$\rho(X, Y) = \frac{COV(X, Y)}{\sigma_X \sigma_Y}, \quad (7)$$

where X and Y represent data of two frames of the echo sequence in matrix form, and σ_X and σ_Y are the standard deviations of the brightness distribution of the respective frames.

Thus, to find similarity between echocardiogram frames we compute the correlation coefficient between the first frame and the rest of the frames. To reduce computational time, we consider the *minimum bounding rectangle* (MBR) of the ellipse that is provided as user input in one of the ED frames of the echo sequence. This produces a correlation graph like one shown in Fig. 3, where the horizontal axis denotes number of frames and the vertical axis gives ρ values. It is expected that, the frames with maximum correlation values within a cardiac cycle in the correlation graph, indicate ED phases of the cardiac cycles. However, as mentioned earlier, cardiac cycles may not be of same duration and hence, it is difficult to find out an interval within which the maximum ρ -value should be searched. Hence, we adopt the following methodology.

3.2 Peak Determination

Let f_1, f_2, \dots, f_n be a subsequence of n frames in the echocardiogram video clip. Let ω be the maxi-

imum expected span of a cardiac cycle in terms of the number of frames. It can be easily understood that ω depends on the physiology of heart and the rate of capturing the echo sequence in digital format. In our computation, we have taken ω as 22. If f_i is an ED frame, the next ED frame should occur between f_{i+1} and $f_{i+\omega}$ frames. As the correlation values will also be higher in the adjacent frames, we search for a local maximum within the frame sequence $\langle f_i + \theta, f_i + \omega \rangle$, where $1 < \theta < \omega$ and $1 \leq i \leq n - \omega$. Let $\mathbb{P}_1, \mathbb{P}_2, \dots, \mathbb{P}_k$ be the k peaks found in this method. These peaks represent the ED frames of the echo sequence. Now, we apply the method described in section 2 with user drawn ellipse initialised at these ED frames.

4 Results

The method proposed in this paper has been implemented on a PC with Pentium III processor and 550 MHz clock under MS Windows-98 environment. It takes around 300 seconds to compute contours of 140 frames of an echocardiogram sequence. The time mentioned includes all bookkeeping tasks, like, file writing etc. In the Fig.4, eight original frames and their corresponding contours tracked by the proposed algorithm are shown. It may easily be observed that, from frame number 128, area of LV starts increasing rapidly. Frame numbers 131 and 132 describe the phase ED. From frame number 133, area value starts decreasing.

However, in the present form, the method fails to demonstrate exactly similar area values in corresponding frames of same phase of different cardiac cycles. The reasons are inexactness of the computed cavity boundary as well as discreteness of area values computed in terms of pixels. Hence, it is difficult to visu-

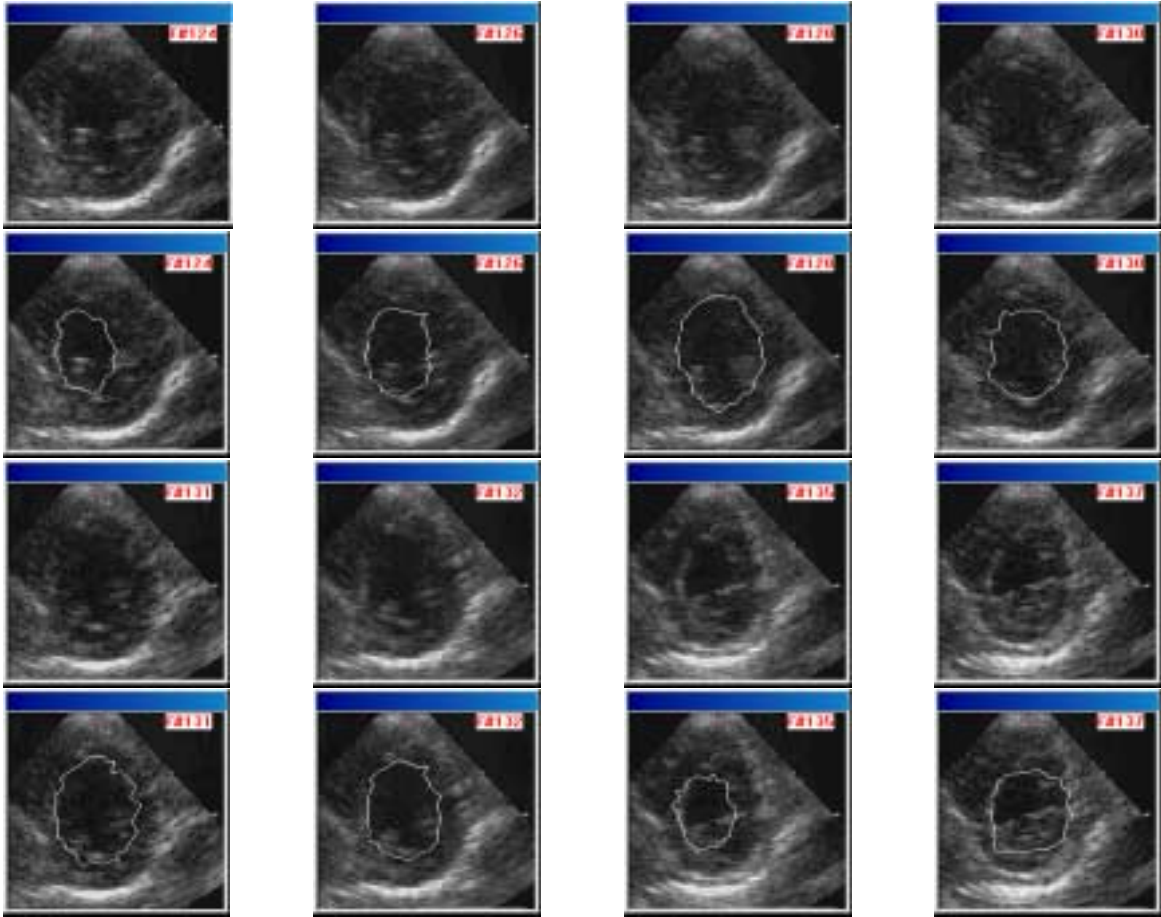


Figure 4: Contours tracked in frames of one cardiac cycle: Top layers show the original frames and bottom layers show corresponding contours tracked (in white colour)

ally comprehend the correspondence of frames among different cardiac cycles, as is seen in Fig. 5(a). In both the plots of Fig. 5, the horizontal axis denotes number of frames and vertical axis denotes area values in number of pixels. On the other hand, the presence of maximum area values, representing the ED frames, is prominent in the area value plot. Since this information is reliable, to alleviate the correspondence problem, we have adopted an averaging scheme to provide acceptable area change information about cardiac motion. In this techniques, we first find the duration of each of different cardiac cycles as the number of frames between two successive peaks in the correlation value plot. The median of these values is taken to be the expected duration, say δ , of a cardiac cycle for the echocardiogram video clip. Finally, we consider area values of frames $f_j, f_{j+\delta}, f_{j+2\delta}, \dots, f_{j+m\delta}$, where

$1 \leq j \leq \delta$, till the number of frames considered in area value plot is less than $(m+1)\delta$, and then for each j , take the median of these values as the expected area of the j^{th} frame of a cardiac cycle. Such an area plot has been shown in Figure 5(b), where values for a cardiac cycle has been repeated seven times to mean that there were seven cycles present in the area plot shown in Fig. 5(a). The pattern illustrated in Fig. 5(b) is similar to the expected pattern of area plot of LV for a healthy patient given in medical literature.

5 Conclusion

In this paper we have addressed the problem of object tracking in echocardiogram images. In our technique, at first, an area of interest around an object is marked by the user in the first frame of the image sequence. Then, an estimate of the object boundary is obtained by a ray-shooting approach. These esti-

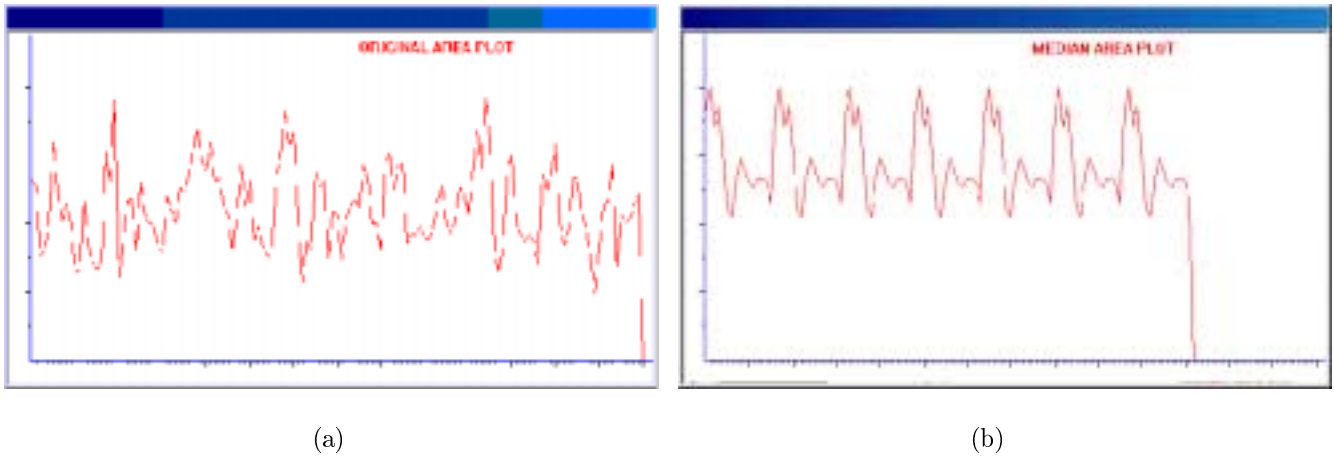


Figure 5: (a) Actual area plot for 140 frames (b) Median area plot over seven cardiac cycles

mates for two subsequent frames are used to adjust the initial contour for each frame. Initial contours are then allowed to converge based on a relaxation-based active contouring algorithm. This method, at its present stage, is able to predict the object movement of LV in an echocardiogram sequence. However, further refinement of this work is required to make the method robust. Nevertheless, this method can be used as an aiding tool in diagnosis of cardiovascular disorders by the cardiologists as it requires less user interaction and is also computationally efficient.

Acknowledgement

We are grateful to Dr. Sankar Mitra, M.D. and other staff members of Eko Heart Foundation, Calcutta for providing us the echocardiogram images and for extending their help to us for this work.

References

- [1] J.E.Perez, A. Waggoner, B. Barzilai, H.E.Melton, J.G.Miller, and B. Sobel, "On-line assessment of ventricular function by automatic boundary detection and ultrasonic backscatter imaging," *Journal of the American College of Cardiology*, vol. 19, pp. 313–320, 1992.
- [2] A. Giachetti, "On line analysis of echocardiographic image sequences," *Medical Image Analysis*, vol. 1, pp. 1–25, 1996.
- [3] J.S.Duncan and N. Ayache, "Medical image analysis: Progress over two decades and the challenges ahead," *IEEE Trans. on Pattern Analysis and Machine Intelligence*, vol. 22, no. 1, pp. 85–106, 2000.
- [4] I. Herlin and N. Ayache, "Features extraction and analysis methods for sequences of ultrasound images," in *Proc. 2nd E.C.C.V.*, pp. 43–55, 1992.
- [5] L. D. Cohen and I. Cohen, "Finite element methods for active contour models and balloons for 2-d and 3-d images," *IEEE Trans. on Pattern Analysis and Machine Intelligence*, vol. 15, pp. 1131–1147, November 1993.
- [6] I. Herlin, D. Breziat, G. Giraudin, C.Nguyen, and C. Graffigne, "Segmentation of echocardiographic images with markov random field," in *Proc. 3rd E.C.C.V.*, pp. 201–206, 1994.
- [7] G. Mailloux and A. B. et al., "Computer analysis of heart motion from two-dimensional echocardiograms," *IEEE Trans. on Biomedical Engineering*, vol. 34, no. 5, p. 356, 1987.
- [8] M. Kass, A. Witkin, and D. Terzopoulos, "Snakes: active contour models," *International Journal of Computer Vision*, vol. 1, no. 4, pp. 321–331, 1987.
- [9] B. Acharya, J. Mukherjee, and A. K. Majumdar, "Two-phase relaxation approach for extracting contours from noisy echocardiogram images," in *Proc. Int'l Conf. Pattern Recog. and Digital Tech. (ICAPRDT99)*, pp. 144–148, 1999.
- [10] P.C.Yuen, G.C.Feng, and J.P.Zhou, "A contour detection method: Initialization and contour model," *Pattern Recognition Letters*, vol. 20, pp. 141–148, 1999.